

APPLICATION NO. 09/826,118

TITLE OF INVENTION: Wavelet Multi-Resolution Waveforms

INVENTOR: Urbain A. von der Embse



Marked up version of amended ABSTRACT OF THE
DISCLOSURE

APPLICATION NO. 09/826,118

TITLE OF THE INVENTION: ~~New~~ Wavelet Multi-Resolution Waveforms

INVENTORS: Urbain ~~Alfred A.~~ von der Embse

5 ABSTRACT OF THE DISCLOSURE

ABSTRACT

A method for designing Wavelets for communications and
radar which combines requirements for Wavelets and finite impulse
response FIR filters including no excess bandwidth, linear
10 performance metrics for passband, stopband, quadrature mirror
filter QMF properties, intersymbol interference, and adjacent
channel interference, polystatic filter design requirements, and
non-linear metrics for bandwidth efficient modulation BEM and
synthetic aperture radar SAR. Demonstrated linear design
15 methodology finds the best design coordinates to minimize the
weighted sum of the contributing LS error metrics for the
respective performance requirements. Design coordinates are
mapped into the optimum FIR symbol time response. Harmonic
design coordinates provide multi-resolution properties and enable
20 a single design to generate Wavelets for arbitrary parameters
which include dilation, down-sampling, up-sampling, time
translation, frequency translation, sample rate, symbol rate,
symbol length, and set of design harmonics. Non-linear
applications introduce additional constraints. Performance
25 examples are linear communications, BEM, and SAR.

~~The present invention describes a new method for the design~~
~~of multi-resolution waveforms to improve system performance,~~
~~design flexibility, applicability, and reduce the costs of~~
30 ~~implementation, compared to the current art. The multi-~~
~~resolution waveform designs are a generalization of Wavelets to~~
~~the Fourier domain. This generalization uses design algorithms~~
~~which include application metrics to improve system performance,~~
~~allows a single design to be used for all scales, and allows~~

~~each design to be characterized by a relatively few parameters. Preliminary simulations indicate that waveform and filter performance can be significantly improved compared to current techniques for communications applications to code division~~
5 ~~multiple access (CDMA) waveforms and filters, communications constant-amplitude bandwidth efficient waveforms, and radar system applications.~~

APPLICATION NO. 09/826,118

TITLE OF INVENTION: Wavelet Multi-Resolution Waveforms

INVENTOR: Urbain A. von der Embse

Currently amended Claims

APPLICATION NO. 09/826,118

INVENTION: ~~New~~ Wavelet Multi-Resolution Waveforms

INVENTORS: Urbain ~~Alfred A.~~ von der Embse

5

CLAIMS

10 WHAT IS CLAIMED IS:

Claim 1. (currently amended) An iterative eigenvalue least-squares LS method for designing digital mother Wavelets at baseband for ~~A means for the design of new multi-resolution~~
15 ~~waveforms and filters, said method comprising steps: in the Fourier domain with properties which~~
power spectral density PSD representative requirements for said

mother Wavelet ψ frequency ω response $\psi_{\omega}(\omega)$ in a multi-channel filter bank, specify

- 20 a) passband frequency range for waveform transmission,
b) stopband spacing between adjacent filters,
c) bounds on ripple over said passband,
d) stopband filter attenuation,
e) rolloff with frequency outside stopband,
25 f) quadrature mirror filters QMF require the sum of said
PSD's for contiguous filter responses to be flat over
deadband which is said stopband,
g) symbol-to-symbol interference ISI,
h) adjacent channel interference ACI,

30 ~~provide extensions of the Wavelet concept to the Fourier domain or equivalently the frequency domain~~

~~provide single waveform designs for all of the waveform s at multiple scales~~

35

~~provide designs which requires a relatively few design
coordinates compared to the FIR time response samples for
the waveform~~

~~provide design methodologies which can incorporate
application metrics to improve the waveform performance
provide designs that allow the use of direct design
methodologies that circumvent the need to solve a Wavelet
iterated filter bank construction to obtain the waveforms
thereby providing improved flexibility to meet the
application goals~~

said LS error metrics to measure said requirements (a)-(h) are
derived as functions of said Wavelet $\psi(n)$ assuming

i) T and $1/T$ are sample interval and sample rate equal to
Nyquist sample rate,

j) ψ is real and symmetric about $n=0$,

k) $n = 0, \pm 1, \dots, \pm ML/2$ digital index over said ψ ,

l) M is interval between contiguous said ψ ,

m) $1/MT$ is said ψ symbol rate and channel-to-channel
separation,

n) L is length of said ψ in units of said M ,

said multiple-resolution properties require said LS metrics
to be constructed as functions of said Wavelet Fourier
harmonics $\psi_k(k)$ with $k=0, \pm 1, \dots, \pm(N_k-1)$ and
 $N_k \geq L$ is a design parameter,

it is sufficient to use positive $n=0, 1, \dots, ML/2$ and $k=0, 1, \dots$
 \dots, N_k-1 since said $\psi(n)$ and $\psi_k(k)$ are real and symmetric,
 $ML/2+1 \times N_k$ matrix bw wherein "x" reads "by" maps $\psi_k(k)$ into
 $\psi(n)$ to within a scale factor by equations

$\psi(n) = \sum_k bw(n+1, k+1) \psi_k(k)$ for $n \geq 0, k \geq 0$,

$bw(n+1, k+1) = 1$ for $n=0$,

$= 2 \cos(2\pi nk/ML)$ otherwise,

$=$ row $n+1$, column $k+1$ element of bw ,

said $\psi(n)$ and $\psi_k(k)$ are converted to column vectors by equations

$h = ML/2+1 \times 1$ column vector of $\psi(n)$ with elements
 $h(1) = \psi(n=0),$
 $h(n+1) = 2\psi(n)$ for $n=1,2,...,ML/2,$
 $h_k = N_k \times 1$ column vector of $\psi_k(k)$ with elements
5 $h_k(1) = \psi_k(k=0),$
 $h_k(k+1) = 2\psi_k(k)$ for $k=1,2,...,N_k-1,$
sawd bw maps h_k into h to within a scale factor by matrix equation
 $h = bw \ h_k,$
LS error metrics for band = passband, stopband, and QMF deadband
10 requirements are derived as quadratic forms in sawd $h,$
sawd LS error metrics are converted by sawd bw mapping into
quadratic forms in sawd h_k equal to $J(\text{band})=h_k'R \ h_k$ wherein
sawd h_k' is the transpose of h_k and sawd R is a real square
symmetric matrix of LS errors in meeting sawd requirements.
15 LS ISI,ACI error metrics $J(\text{ISI}),J(\text{ACI})$ are derived as non-linear
quadratic forms in h and converted by sawd bw matrix to the
non-linear quadratic form in h_k equal to $J(\text{ISI})=\delta E'\delta E,$
 $J(\text{ACI})=2\delta E'\delta E$ wherein $\delta E = AHh_k$ is a column vector and
matrix "A" in the matrix product AH is a function of sawd h
20 hereby introducing sawd non-linearity, and sawd AH differ
for ISI and ACI error metrics,
LS cost function J is the weighted sum of sawd LS error metrics
 $J = \sum w(\text{LS metric}) \ J(\text{LS metric})$
with summation over sawd LS metrics= passband, stopband,
25 QMF deadband, ISI, ACI with normalized weights
 $\sum w(\text{LS metric})=1,$
sawd weights are free design parameters,
sawd iterative eigenvalue LS algorithm at each step finds the
optimum eigenvalue and eigenvector which minimize sawd
30 quadratic form J in h_k for a constant sawd "A",
sawd eigenvector is the optimum h_k which minimizes sawd J and
sawd bw equation derives the corresponding optimum h which
minimizes sawd $J,$

step 1 in said iterative algorithm finds said optimum eigenvalue,
eigenvector, h_k , h of J reduced by deleting said non-linear
ISI and ACI LS quadratic error metrics,

said h is used to evaluate said "A" matrices for step 2,

5 step 2 finds said optimum eigenvalue, eigenvector, h_k , h for
minimum J using said "A" from step 1,

said h is used to evaluate said "A" for step 3,

steps 3,4, etc. continue until said minimum J converges to a
steady value and,

10 said optimum $\psi_k(k)$ uses said bw to calculate optimum $\psi(n)$ for
implementation as said Wavelet FIR digital waveform and
filter time response.

15

Claim 2. (currently amended) An LS method for designing digital
mother Wavelets at baseband for multi-resolution waveforms and
filters, 2. A means for the design of multi-resolution waveforms
and filters in the frequency domain or equivalently the Fourier
20 of the t - f space for waveform and filter applications, with
properties which said method comprising steps:

said PSD waveform representative requirements and assumptions
are recited in (a)-(n) in Claim 1,

said multiple-resolution properties require said LS metrics

25 to be constructed as functions of said $\psi_k(k)$,

said LS error metrics for said passband, stopband, and QMF
deadband requirements are derived as squared vector norm
functions of said h and converted by said bw matrix into

$J(\text{band}) = \|Bh_k\|^2$ wherein $\|Bh_k\|$ is the vector norm of the

30 column vector Bh_k and said B is the matrix of LS errors in
meeting said requirements and wherein said squared vector
norm is suitable for LS optimization,

~~provide a means for single design to be used for all of the waveforms at the multiple resolutions or frequency bands~~

~~provide a means for designs that require a relatively few design coordinates compared to the number of digital samples covered by the Wavelet~~

~~provide a means for the designs to include frequency and time application metrics to improve the waveform performance~~

LS ISI,ACI error metrics $J(\text{ISI}), J(\text{ACI})$ are derived as squared

vector norm functions equal to $J(\text{ISI}) = \|\delta E\|^2$, $J(\text{ACI}) = 2\|\delta E\|^2$

using said column vectors $\delta E = A H h_k$ in claim 1,

LS cost function J is said weighted sum of said LS error metrics

equal to $J = \sum w(\text{LS metric}) J(\text{LS metric})$ defined in claim 1,

an LS gradient search algorithm finds optimum $h_k(k)$ to

minimize J ,

step 1 of said LS gradient search algorithm uses a Remez-

exchange algorithm to find said optimum $h_k(k)$ for said J

reduced to said passband and stopband LS metrics,

~~provide a means to use direct design methodologies in the frequency time domain c for all of the waveforms and filters for the multiple frequency bands~~

step 2 uses the estimated $h_k(k)$ from step 1 to initialize said gradient search,

step 3 selects one of several available gradient search

algorithms, gradient search parameters, and stopping rules,

step 4 implements said algorithm, parameters, and stopping rule

selected in step 3 to derive said optimum $h_k(k)$ to minimize J and,

said optimum h_k uses said bw to calculate optimum $\psi(n)$ for

implementation as said Wavelet FIR digital waveform and filter time response.

Claim 3. (currently amended) Wherein said mother Wavelet in Claims 1,2 generates multi-resolution dilated Wavelets, comprising steps and design:

5 said Wavelet parameters are

- a) scaling parameter p dilates sampling by factor 2^p equivalent to sub-sampling by factor 2^p ,
- b) translation parameter q translates said ψ by qM digital samples,
- 10 c) frequency offset k is set by design,
- d) symbol repetition interval said M remains constant,
- e) Wavelet length said L in units of said M remains constant,

step 1 uses said design harmonics ψ_k to generate said FIR time response $\psi(n_p)$ at baseband with said bw equation

15
$$\psi(n_p) = \sum_k bw(n_p+1, k+1) \psi_k(k)$$

recited in claim 1 with

$$bw = 2 \cos(2\pi n_p k / ML) \text{ for } n_p > 0$$

wherein $n_p = n/2^p$ is n sub-sampled or equivalently dilated

20 by the factor 2^p ,

step 2 uses said $\psi(n_p)$ to construct said multi-resolution Wavelet $\psi_{p,q,M,L,k}$ with equation

$$\psi_{p,q,M,L,k} = 2^{(-p/2)} \psi(n_p - qM) \exp(j2\pi kn_p / ML)$$

which is said FIR time response for parameters p,q,M,L,k

25 wherein the subset p,M,L are the scale parameters,

~~A method for the design of multi-resolution waveforms which allows Fourier domain techniques to be used. Properties can include some or more of the listed properties in (1) and (2)~~

30 design of said multi-resolution Wavelet includes

- f) said T for n is increased to $T2^p$ for n_p ,
- g) said $1/T$ is reduced to $1/T2^p$,

- h) said ψ symbol rate $1/MT$ equal to said channel-to-channel separation is reduced to $1/MT2^p$ in Hz and,
i) said ψ length $(ML+1)T$ in seconds is stretched to $(ML+1)T2^p$ in seconds.

5

Claim 4. (currently amended) Wherein said mother Wavelet in claims 1,2 generates multi-resolution constant sample rate dilated Wavelets, comprising steps and design:
said Wavelet parameters are

- a) said p dilates said ψ to increase said length from $ML+1$ to M_pL+1 where $M_p=M2^p$ is the dilated interval between contiguous ψ 's,
b) said q translates said ψ by qM_p digital samples,
c) said k is set by design,
d) said $M_p=M2^p$ is dilated M ,
e) said L remains constant,

step 1 uses said design harmonics ψ_k to generate said FIR time response $\psi(n_p)$ at baseband with said bw equation

$$\psi(n) = \sum_k bw(n+1, k+1) \psi_k(k)$$

recited in claim 1 with

$$bw = 2 \cos(2\pi nk/M_pL) \text{ for } n>0,$$

step 2 uses said $\psi(n)$ to construct said multi-resolution Wavelet

$\psi_{p,q,M,L,k}$ with equation

$$\psi_{p,q,M,L,k} = 2^{(-p/2)} \psi(n-qM_p) \exp(j2\pi kn/M_pL)$$

which is said FIR time response for parameters p,q,M,L,k , design of said multi-resolution Wavelet includes

- f) said T remains constant,
g) said $1/T$ remains constant,
h) said ψ symbol rate $1/MT$ equal to said channel-to-channel separation is reduced to $1/M_pT=1/MT2^p$ in Hz and,
i) said ψ length $(ML+1)T$ in seconds is stretched to

(ML2^{p+1})T in seconds.

5

~~A method for the design of multi-resolution waveforms which
can incorporate Fourier domain techniques into design
methodologies which can include analytical and iterated
filter bank construction design techniques.~~

10

Claim 5. (currently amended) Wherein said mother Wavelet in
claims 1,2 generates multi-resolution up-sampled Wavelets,

15 comprising steps and design:

said Wavelet parameters are

a) said p up-samples said digital sampling rate 1/T to 2^p/T,

b) said q translates said ψ by qM digital samples,

c) said k is a design parameter,

20 d) said M is constant

e) said L is constant

step 1 uses said design harmonics $h_{f_l} \psi_k$ to generate said FIR

time response $\psi(n_p)$ at baseband with said equation

$$\psi(n_p) = \sum_k bw(n_p+1, k+1) \psi_k(k)$$

25 recited in claim 1 with

$$bw = 2 \cos(2\pi n_p k / ML) \text{ for } n_p > 0$$

wherein n_p is n up-sampled by the factor 2^p and defined
by equations

$$n_p = n p + n 2^p$$

30 $n p = 0, 1, 2, \dots, 2^p - 1$

wherein $n p$ is the index over the additional samples added
to each sample n by said up-sampling,

step 2 uses said $\psi(n_p)$ to construct said multi-resolution Wavelet

$\Psi_{p,q,M,L,k}$ with equation

$\Psi_{p,q,M,L,k} = 2^{(-p/2)} \psi(n_p - qM) \exp(j2\pi kn_p/ML)$
which is said FIR time response for parameters p,q,M,L,k ,

5

~~A method for the analysis and design of multi-resolution waveforms using Fourier domain techniques which take advantage of the new invention disclosures on the characterization and design of multi-resolution waveforms in the Fourier domain.~~

10

design of said multi-resolution Wavelet includes

f) said T is decreased to $T/2^p$,

g) said $1/T$ is increased to $2^p/T$,

h) said ψ symbol rate $1/MT$ equal to said channel-to-channel

15

separation is increased to $2^p/MT$ in Hz and,

i) said ψ length $(ML+1)T$ in seconds is reduced to

$(ML + 1)T/2^p$ in seconds.

20

Claim 6. (currently amended) Wherein said multi-resolution Wavelets in Claims 1-5 have properties comprising:
said scale parameters p,M,L and said design parameter $1/T$ specify
25 said multi-resolution Wavelets at baseband and said q,k
specify time,frequency translations from baseband,
said design harmonics $\psi_k(k)$ of mother Wavelet are said design
coordinates for multi-resolution Wavelets,
said design harmonics $\psi_k(k)$ use said bw matrix to generate said
30 multi-resolution Wavelet baseband time response $\psi(n)$ for
dilation, dilation of Wavelet length, and up-sampling as
recited in Claims 3-5 and which is translated in time and
frequency to said multi-resolution Wavelet $\Psi_{p,q,M,L,k}$.

said design harmonics $\psi_k(k)$ are few in number compared to said $\psi(n)$,

said ψ is designed to support a bandwidth-time product $B_f T = 1 + \alpha$ with no zero excess bandwidth $\alpha = 0$,

5 said multi-resolution Wavelets are designed to behave like an accordion in that at different scales said Wavelets are stretched and compressed versions of the mother Wavelet with appropriate time and frequency translation,

10 ~~A new formulation in (5) for multi-resolution waveform as a function of the de multi-resolution waveform which adds the concept of a frequency index that allows the multi-resolution waveform to be placed arbitrarily throughout the t-f space thereby 1) avoiding the restrictions of the Wavelet iterated~~
15 ~~filter construction for tiling a t-f space, and 2) allowing the new multi-resolution waveforms to be used for multi-resolution communications and for bandwidth-on-demand communications application, in place of traditional Wavelets.~~

said optimization techniques in claims 1,2 assume said $\psi(n)$

20 symmetric about $n=0$ and are applicable to other arrangements of $\psi(n)$ with self-evident modifications,

optimization algorithms for finding said optimum set of $\psi_k(k)$

use linear LS waveform and filter design methods recited in claims 1,2 and also use other methods and,

25 said linear waveform and filter LS design methods can be modified to design waveforms for applications including bandwidth efficient modulation BEM and synthetic aperture radar SAR.

APPLICATION NO. 09/826,118

TITLE OF INVENTION: Wavelet Multi-Resolution Waveforms

INVENTOR: Urbain A. von der Embse

Marked up version of SUBSTITUTE SPECIFICATION

APPLICATION NO. 09/826,118

TITLE OF INVENTION: ~~New~~ Wavelet Multi-Resolution Waveforms

INVENTOR: Urbain Alfred A. von der Embse

5

BACKGROUND OF THE INVENTION

I. Field of the Invention

10 ~~TECHNICAL FIELD~~

The present invention relates to CDMA (Code Division Multiple Access) cellular telephone and wireless data communications with data rates up to multiple T1 (1.544 Mbps) and higher (>100 Mbps), and to optical CDMA. Applications are
15 mobile, point-to-point and satellite communication networks. More specifically the present invention relates to a new and novel means for a new approach to the design of waveforms and filters using mathematical formulations which generalize the Wavelet concept to communications and radar.

20

~~CONTENTS~~

~~BACKGROUND ART~~ page 1

~~SUMMARY OF INVENTION~~ page 8

~~BRIEF DESCRIPTION OF DRAWINGS AND PERFORMANCE DATA~~

25 page 10

~~DISCLOSURE OF INVENTION~~ page 11

~~REFERENCES~~ page 33

~~DRAWINGS AND PERFORMANCE DATA~~ page 35

30

~~BACKGROUND ART~~

II. Description of the Related Art

Multi-resolution waveforms used for signaling and/or
5 filters and which are addressed in this invention are defined to
be waveforms of finite extent in time and frequency, with scale
and shift properties of multi-resolution over the time-frequency
(t-f) space. These waveforms can also be referred to as multi-
scale waveforms, and include multi-rate filtering and the
10 Wavelet as special cases. The emphasis will be on digital
design and applications with the understanding that these multi-
resolution waveforms are equally applicable to analog design and
applications.

15 Background art consists of the collection of waveform and
filtering design techniques which can be grouped into six broad
categories. These categories are: C1) least squares (LS) design
algorithms for filters and waveforms that design to
specifications on their frequency response, C2) analytic
20 filters and waveforms which are specified by a few free design
parameters that can be sub-categorized into current applications
and primarily theoretical studies, C3) combinations of C1 and
C2 for greater flexibility in meeting communications and radar
performance goals, C4) special design techniques to control the
25 noise levels from intersymbol interference (ISI) and adjacent
channel interference (ACI) in the presence of timing offsets for
multiple channel applications, C5) Wavelet filter design using
scaling functions (iterated filter banks) as the set of design
coordinates or basis functions, C6) filter and waveform design
30 techniques for non-linear channels and in particular for
operation in the non-linear and saturation regions of a high
power amplifier (HPA) such as a traveling wave tube (TWT) or a
solid state amplifier, and C7) LS dynamic filters derived from
discrete filtering and tracking algorithms that include adaptive
35 equalization for communications, adaptive antenna filters,

Wiener filters, Kalman filters, and stochastic optimization filters.

Category C1 common examples of LS digital filter design are
5 the eigenvalue algorithm in "A New Approach to Least-Squares FIR
Filter Design and Applications Including Nyquist Filters" [7] and
the Remez-Exchange algorithm in "A Computer Program for Designing
Optimum FIR Linear Phase Filters". [8]. The eigenvalue algorithm
is a direct LS minimization and the Remez-Exchange can be
10 reformulated as an equivalent LS gradient problem through proper
choice of the cost function. Both LS algorithms use the FIR
(finite impulse response) digital samples as the set of design
coordinates. LS design metrics are the error residuals in
meeting their passband and stopband ideal performance as shown
15 in FIG. 3. Category C2 common examples of analytical waveforms
and filters for system applications are the analog Chebyshev,
Elliptic, Butterworth, and the digital raised-cosine, and square-
root raised-cosine. For theoretical studies, common examples
are polyphase multirate filters, quadrature mirror filters
20 (QMF), and perfect reconstruction filters. Although these
theoretical studies have yet to yield realizable useful filters
for system applications, their importance for this invention lies
in their identification and application of ideal performance
metrics for filter designs. Category C3 common digital example
25 is to start with the derivation of a Remez-Exchange ~~finite
impulse response (FIR)~~ filter and then up-sample and filter with
another bandwidth limiting filter. This results in an FIR over
the desired frequency band that is larger than available with the
Remez-Exchange algorithm and with sidelobes that now drop off
30 with frequency compared to the flat sidelobes of the original
Remez-Exchange FIR. A category C4 common example is to select
the free parameters of the category C3 filter in order to
minimize the signal to noise power ratio of the data symbol (SNR)
losses from the ISI, ACI, and the non-ideal demodulation. A
35 second common example is start with a truncated pulse whose

length is short enough compared to the symbol repetition interval, to accommodate the timing offsets without significant impact on the ISI and ACI SNR losses. This shortened pulse can then be shaped in the frequency domain.

5

Category C5 Wavelet filter design techniques discussed in the next section will serve as a useful reference in the disclosure of this invention. Category C6 common example is the Gaussian minimum shift keying (GMSK) waveform. This is a
10 constant amplitude phase encoded Gaussian waveform which has no sidelobe re-growth through a non-linear or saturating high power amplifier (HPA). Category C7 common examples are the adaptive equalization filter for communication channels, the adaptive antenna filter, and the Kalman filter for applications including
15 target tracking and prediction as well as for equalization and adaptive antennas.

Minimizing excess bandwidth in the waveform and filter design is a key goal in the application of the C1,...,C6 design
20 techniques for communications and radar. Excess bandwidth is identified as the symbol α in the bandwidth-time product $BT_s=1+\alpha$ where the two-sided available frequency band is B and the symbol repetition interval is T_s . Current performance capability is represented by the use of the square-root raised cosine (sq-rt
25 rc) waveform with $\alpha= 0.22$ to 0.4 as shown in FIG. 46. The goal is to design a waveform with $\alpha=0$ within the performance constraints of ISI, ACI, passband, sideband, and passband ripple. This goal of eliminating the excess bandwidth corresponds to the symbol rate equal to the available frequency band $1/T_s =$
30 $B/(1+\alpha) = B$ for $\alpha=0$. This symbol rate $1/T_s=B$ is well known to be the maximum possible rate for which orthogonality between symbols is maintained. A fundamental performance characteristic of our new waveform designs is the ability to eliminate excess bandwidth for many applications.

Scope of this invention will include all of the waveform and filter categories with the exception of category C4 special design techniques and category C7 LS dynamic filters. Emphasis will be on the category C5 Wavelets to establish the background art since Wavelets are multi-resolution waveforms that can eliminate the excess bandwidth and have known design algorithms for FIR waveforms and filters. However, they do not have a design mechanism that allows direct control of the ISI, ACI, passband, sideband, and passband ripple. Category C2 theoretical studies also eliminate the excess bandwidth. However, they are not multi-resolution waveforms and do not have realizable FIR design algorithms. So the emphasis in background art will be on Wavelets whose relevant properties we briefly review.

Wavelet background art relevant to this invention consists of the discrete Waveform equations and basic properties, application of Wavelets to cover a discrete digital time-frequency (t-f) signal space, and the design of Wavelets using the iterated filter construction. Wavelets are waveforms of finite extent in time (t) and frequency (f) over the t-f space, with multi-resolution, scaling, and translation properties. Wavelets over the analog and digital t-f spaces respectively are defined by equations (1) and (2) as per Daubechies's "Ten Lectures on Wavelets", Philadelphia: SIAM, 1992

~~reference [1].~~

Continuous wavelet

$$\psi_{a,b}(t) = |a|^{-1/2} \psi\left(\frac{t-b}{a}\right) \quad (1)$$

Discrete wavelet

$$\psi_{a,b}(n) = |a|^{-1/2} \psi\left(\frac{n-b}{a}\right) \quad (2)$$

where the two index parameters "a,b" are the Wavelet dilation and translation respectively or equivalently are the scale and shift. The ψ is the "mother" wavelet and is a real and symmetric localized function in the t-f space used to generate the doubly indexed Wavelet ψ_{ab} . The scale factor " $|a|^{-1/2}$ " has been chosen to keep the norm of the Wavelet invariant under the parameter change "a,b". Norm is the square root of the energy of the Wavelet response. The Wavelets $\psi_{a,b}$ and ψ are localized functions in the t-f space which means that both their time and frequency lengths are bounded. The discrete Wavelet has the time "t" replaced by the equivalent digital sample number "n" assuming the waveform is uniformly sampled at "T" second intervals.

Wavelets in digital t-f space have an orthogonal basis that is obtained by restricting the choice of the parameters "a,b" to the values $a=2^{-p}$, $b=qM2^p$ where 'p,q' are the new scale and translation parameters and "M" is the spacing or repetition interval $T_s=MT$ of the Wavelets (which from a communications viewpoint are symbols) at the same scale "p". Wavelets at "p,q" are related to the mother Wavelet by the equation {1}

$$\psi_{p,q}(n) = 2^{-p/2} \psi(2^{-p}n - qM) \quad (3)$$

where the mother Wavelet is a real and even function of the sample coordinates. The orthonormality property means that these Wavelets satisfy the orthogonality equation with a correlation value equal to "1".

$$\sum_n \psi_{p,q} \psi_{k,m} = 1 \text{ iff both } p = k \text{ and } q = m$$

$$= 0 \text{ otherwise} \quad (4)$$

Wavelet representation of a digital t-f space starts with selecting an N sample time window of a uniform stream of digital samples at the rate of 1/T Hz (1/second) equivalent to a "T" second sampling interval. The N point or sample t-f space in FIG. 1 illustrates a Wavelet representation or "tiling" with Wavelets that are designed analytically or by an iterated filter construction.

The t-f space in FIG. 1 is partitioned or covered or tiled by a set of Wavelet subspaces $\{W_p, p = 0, 1, \dots, m-1\}$ where $N = 2^m$. Each Wavelet subspace W_p at scale "p" consists of the set of Wavelet time translations $\{q = 0, 1, \dots, N/2^{p+1}-1\}$ over this subspace. These Wavelet subspaces are mutually orthogonal and the Wavelets within each subspace are mutually orthogonal with respect to the time translates. This N-point t-f space extends over the time interval from 0 to (N-1)T where T is the digital sampling interval, and over the frequency interval from 0 to (N-1) in units of the normalized frequency fNT.

The iterated filter bank in FIG. 2 is used to generate the Wavelets which cover the t-f space in FIG. 1. Each filter stage consists of a high pass filter (HPF) and a low pass filter (LPF). Output of the LPF is subsampled by 2 which is equivalent to decimation by 2. This t-f space is an N-dimensional complex vector metric space V. At stage m in the iterated filter bank, the remaining t-f space V_{m-2} is partitioned into V_{m-1} and the Wavelet subspace W_{m-1} .

Scaling functions and Wavelets at each stage of this filter bank satisfy the following equations

$$\begin{aligned}
\psi(n) &= 2^{-1/2} \sum_q h_q \varphi(2n-q) \quad \forall q \\
\varphi(n) &= 2^{-1/2} \sum_q g_q \varphi(2n-q) \quad \forall q
\end{aligned}
\tag{5}$$

5 where φ is the scaling function, ψ is the Wavelet, HPF_p coefficients are $\{h_q, \forall q\}$, LPF_p coefficients are $\{g_q, \forall q\}$, and the equations apply to the stages $0, 1, \dots, m-1$. Identifying the scale parameter and using the previous Wavelet formulations enable these equations to be rewritten for stages $p=0, 1, \dots, m-1$
10 as

$$\begin{aligned}
\psi_p &= \sum_q h_q \varphi_{p-1,q} \quad \forall p \\
\varphi_p &= \sum_q g_q \varphi_{p-1,q} \quad \forall p
\end{aligned}
\tag{6}$$

For our application the HPF_p and LPF_p are quadrature mirror
15 filters (QMF) with perfect reconstruction. This means they cover the subspace V_p with flat responses over the subband frequency including the edges of the frequency subband, and the HPF_p coefficients are the frequency translated coefficients for the LPF_p : $\{g_q = (-1)^q h_q, \forall q\}$.

20

Wavelet design using iterated filter bank starts with the selection of the scaling functions. Starting with a primitive scaling function such as the one proposed by Daubechies-[1],—one can use the iterated filter construction given by equations (5)
25 and (6) to derive successive approximations to a desired scaling function which has properties that have been designed into it by the selection of the filter coefficients $\{g_q, \forall q\}$ at each level of iteration. The Wavelets can be derived from these scaling

functions using the iterated filter construction or scaling equations (5) and (6).

Another use of the iterated filter construction is to design the scaling functions as Wavelets thereupon ending up with a larger set of Wavelets for multi-resolution analysis and synthesis as illustrated by Coifman's Wavelets in "Wavelet analysis and signal processing". [2]. ~~Design examples abound in the open literature and the recent publications [3], [4], [5], [6] are representative illustrations of the diverse applications of Wavelets.~~

~~SUMMARY OF INVENTION~~

SUMMARY OF THE INVENTION

This invention ~~is a new approach to~~for the design of new Wavelet multi-resolution waveforms ~~that~~—improves their performance for engineering and scientific applications, and in particular for applications to communications and radar. Current practice is to 1) design traditional multi-resolution waveforms in the time domain using metrics which specify frequency performance and without consideration of Wavelet properties, ~~and~~ or to 2) design Wavelet multi-resolution waveforms using the time-domain iterated multi-resolution filtering approach with a set of scaling functions used to perform the filtering and without direct considerations of the frequency performance. These two separate design approaches yield fundamentally different waveforms. ~~Our new~~This invention provides a means to combine these two approaches to generate a new multi-resolution waveform with the best properties of the traditional multi-resolution waveforms and the Wavelet multi-resolution waveform.

~~Our~~ This invention introduces ~~the new~~ innovations for the design of our new waveform that 1) include the ISI (intersymbol interference), ACI (adjacent channel interference), and QMF (quadrature mirror filter) requirements into the design algorithm along with non-linear modifications to the traditional passband and stopband frequency requirements which are used in the Remez-Exchange and eigenvalue LS algorithms ~~in references [8], [7]~~ respectively, 2) select the frequency harmonics as the design coordinates, 3) use an appropriate subset of the available Fourier domain frequency harmonics as the design coordinates with the property that this subset of coordinates is a basis for the multi-resolution waveform design, and 4) design the multi-resolution waveform for no excess bandwidth $\alpha=0$.

These innovations support the development of our ~~new~~ waveforms 1) that are generalizations of Wavelets in the frequency domain using a means which makes them useful for communications and radar over their t-f space, 2) that can be designed to be an orthonormal basis or orthonormal set of coordinates over the available frequency bandwidth with the implicit property that the excess bandwidth vanishes $\alpha=0$, to within the accuracies allowed by communication and radar design implementations, and 3) that have multi-scale properties which allow a single dc waveform design to be used to uniquely define the complete set of ~~new~~ waveforms over the t-f space for multi-scale applications. Specific design algorithm examples developed in this invention disclosure are the LS design algorithms that use eigenvalue and gradient search techniques in the frequency domain to find the best waveform design which minimizes the corresponding LS error residual cost function that is a weighted linear sum of the residual error metrics.

Waveform performance calculated in this invention disclosure from the application of these LS design algorithms, demonstrates the capability of this invention to provide a means to design waveforms that are improved over current practice.

5 There are other algorithmic design algorithms which can be realized by modifications to this invention. An example given in this invention disclosure is the modification of these LS algorithms for application to constant amplitude bandwidth efficient (BEM) waveforms for communications.

10

BRIEF DESCRIPTION OF THE DRAWINGS AND THE PERFORMANCE DATA

~~BRIEF DESCRIPTION OF DRAWINGS AND PERFORMANCE DATA~~

15 The above-mentioned and other features, objects, design algorithms, and performance advantages of the present invention will become more apparent from the detailed description set forth below when taken in conjunction with the drawings and performance data wherein like reference characters and numerals denote like

20 elements, and in which:

FIG. 1 is a Wavelet ~~an~~-N-point t-f space extending over the time interval $(0, (N-1)T]$ and the frequency interval $(0, (N-1)/NT]$, which is tiled or covered by a set of orthonormal

25 Wavelets at the scales $p=0,1,...,m-1$.

FIG. 2 is a Wavelet iterated filter bank used to generate the set of Wavelets which tile or cover the t-f space in FIG. 1.

30 FIG. 3 illustrates the power spectral density (PSD) of our ~~new~~-waveform at dc, and the set of stopband and passband design requirements.

FIG. 4 is the flow diagram of the LS metrics and cost functions and the final cost function used to find the optimal LS solution for our waveform.

5 FIG. 5 is flow diagram for the LS recursive solution algorithm to find the optimal harmonic coordinates that define the LS solution for our waveform.

10 FIG. 6 plots the dc PSD in dB units for ~~the~~our new waveforms vs. the normalized frequency fT_s for ~~the~~our new waveform designed with the LS algorithms and for the sq-rt r-c waveforms with excess bandwidth parameter $\alpha = 0.22, 0.40$.

15 FIG. 7 plots the dc PSD in dB units ~~for our waveforms vs.~~ the normalized frequency fT_s for ~~the~~our new waveform designed with modifications to the LS algorithms for application to constant amplitude BEM communications, and for a Gaussian
20 minimum shift keying (GMSK) waveform.

25 FIG. 8 plots the amplitude of the dc radar ambiguity function vs. the normalized frequency fT_p and normalized time tT_c where the pulse time T_p and chip time T_c are both equal to the communications symbol interval T_s for this example, for ~~the~~our new waveform and an unweighted chirp waveform.

30

35

~~DISCLOSURE OF INVENTION~~

DISCLOSURE OF THE INVENTION

5

New waveforms in this invention disclosure are generalizations of Wavelets in t-f space which enable them to be useful for communications and radar applications. This
10 generalization is accomplished by 1) the ~~addition~~ introduction of a frequency translation, by 2) ~~relaxing~~ changing the orthonormality condition in equation (4) to apply to waveforms within the same space {q} and over the scales {p} with the inclusion of the frequency translation, and 3) by their
15 characterization and design in the Fourier domain.

With frequency translation the analytical formulation of these new waveforms as a function of the baseband or mother waveform centered at dc_{-} ($-dc_{-}$ refers to the origin $f=0$ of the
20 frequency space) becomes

~~New waveform as a function of dc waveform~~

$$\psi_{p,q,r}(n) = 2^{-p/2} \psi(2^{-p}n - qM) e^{i2\pi f_c(p,r)nT} \quad (7)$$

25

where $f_c(p,r)$ is the center frequency of the frequency translated dc waveform, at scale "p" and frequency index "r". The purpose of the frequency index "r" is to identify the center frequencies
30 of the waveforms at the scale "p" in the t-f space. ~~The dc or baseband or mother waveform is the generalization of the mother Wavelet for multi-resolution waveforms.~~

These waveforms satisfy the complex orthonormality equations

~~Orthogonality equations~~

$$\sum_n \psi_{p,q,r} \psi_{k,m,v}^* = 1 \text{ iff } p = k \text{ and } q = m \text{ and } r = v$$

$$= 0 \text{ otherwise} \quad (8)$$

where "*" is conjugation, and are generalizations of the orthonormality equations for the analytical Wavelets in (4).

10 ~~The new waveforms in equation (7) expand the Wavelet analytical formulation to include a frequency variable. Wavelets are functions of the scale and translation parameters "p,q". The concept of an additional parameter to provide an added degree of flexibility in their tabulation was first introduced by~~
 15 ~~the Coifman library of Wavelets [2] which use an oscillation parameter for tabulation that roughly corresponds to the frequency of oscillation of the Wavelets. The frequency variable together with the Fourier domain design are entirely new means for deriving these new waveforms as generalization of the~~
 20 ~~traditional Wavelets and their modification with the added parameter in [2].~~

25 ~~New~~ Our new waveforms are generalizations of Wavelets in the frequency domain using a means which makes them useful for communications and radar in the t-f space. The basis vectors for this metric space V consist of a subset of the admissible set of scaled and translated waveforms $\{\psi_{p,q,r}, \forall p,q,r\}$ derived from the dc waveform ψ as per equation (7). An admissible waveform is any combination that covers $V=t-f$ space. We are interested in
 30 the Fourier domain representation of the dc waveform ψ in V , and in particular in a subset of the discrete Fourier transform

(DFT) harmonic coefficients over the Fourier domain which we intend to use as the design coordinates. Starting with the z-transform and continuous Fourier transform, the DFT harmonic coefficients are defined by the following equations

5

DFT Harmonic Coefficients

(9)

10

$$\begin{aligned}\psi(z) &= \sum_n \psi(n) z^{-n} \quad \text{z-transform} \\ \psi(\omega) &= \sum_n \psi(n) e^{-i\omega n} \quad \text{Fourier transform} \\ \psi_k &= \sum_n \psi(n) W_{N'}^{kn} \quad \text{DFT harmonic coefficients for } \forall k\end{aligned}$$

where

$$\begin{aligned}\psi(\omega) &= (1/N') \sum_k \Psi_k \sum_n e^{i(2\pi k/N' - \omega)n} \\ &= \sum_k \psi_k \sin((\omega/2 - \pi k/N')N') / N \sin(\omega/2 - \pi k/N') \\ &= \sum_k \psi_k [\text{Harmonic interpolation for "k"}]\end{aligned}$$

$$W_{N'}^{kn} = e^{i2\pi kn/N'}$$

{k} = DFT frequency or harmonic coefficients such that $f_k = k/N'T$

where f_k is the harmonic frequency corresponding to "k"

N' = length of $\psi(n)$

15

where $\Psi(\omega) = |\psi(\omega)|^2$ is the power spectral density of the dc waveform. These equations define the frequency representation of our new waveforms in terms of the available set of harmonic coefficients, which set is considerable larger than required for most applications.

20

~~New~~ Our new waveforms are an orthonormal basis with no excess bandwidth, ~~are properties that we will demonstrate.~~ Orthonormality and no excess bandwidth ~~are properties which are~~

asymptotically approached ~~by our new waveforms~~ to within design accuracies inherent in communications and radar. To proceed we need to identify the structure of the dc waveform in V . We start with definitions for the parameters and coordinates in the following equation (10). The waveforms derived from the dc waveform will be designed to be orthogonal over both time translates " MT " and frequency translates " $1/LTMT$ " which respectively correspond to the Wavelet symbol spacing $T_s=MT$ and the adjacent channel spacing $1/T_s$. This means the orthogonal spacing of the waveforms in V are at the time-frequency increments $(MT, 1/LTMT) = (T_s, 1/T_s)$. In the interests of constructing our ~~new~~ orthonormal multi-resolution waveforms to cover V it will be convenient to assume that M, L are powers of 2. We need the following definitions for the parameters and coordinates.

Parameters and Coordinates

(10)

20

N' = Length of ψ which is an even function about the center and
 which spans an odd number of points or samples
 = $ML + 1$ where M, L are assumed to be even functions for
 convenience of this analysis
 = Number of points of ψ
 M = Sampling interval for ψ
 = Spacing of ψ for orthogonality
 L = Length of ψ in units of the sample interval M
 = Stretching of ψ over L sample intervals
 n = $n_0 + n_1 M$
 = partitioning into an index n_0 over the sample
 length $n_0 = 0, 1, \dots, M - 1$ and an index $n_1 = 0, 1, \dots, L - 1$
 over the sample intervals
 k = $k_0 + k_1 L$
 = partitioning into an index k_0 over the harmonic
 frequencies $k_0 = 0, 1, \dots, L - 1$ corresponding to the
 stretching and an index $k_1 = 0, 1, \dots, M$ over the harmonics
 frequencies corresponding to the admissible frequency
 slots for ψ

The harmonic design coordinates are selected using the
 following observation. For most applications and in the following
 development it is assumed that the waveforms are spectrally
 5 contained in the frequency interval $1/4T - MT$ corresponding to the
 frequency spacing. This suggests the harmonic design coordinates
 be restricted to the subset of L harmonics $\{k_0=0, 1, \dots, L-1\}$
 covering this spacing. These L harmonics correspond to the
 stretching of the mother waveform over the L repetition
 10 intervals.

Obviously, for some applications as will be demonstrated
 later, the spectral containment is spread out over several $1/4T$
 frequency increments whereupon one must increase the subset of
 15 design harmonics to possibly $2L, 3L$ or larger.

The DFT equations for the dc waveform in (9) when rewritten in terms of the L harmonic design coordinates $\{\psi_{k_0}, \forall k_0\}$ become:

5

DFT equations for dc waveform

$$\psi_{k_0} = \sum_n \psi(n) W_N^{-k_0 n} \quad \text{harmonic design coordinates}$$

$$\psi(n) = (1/N') \sum_{k_0} \Psi_{k_0} W_N^{k_0 n} \quad \text{new waveform defined in terms} \quad (11)$$

10

of the L harmonic design coordinates $\{\psi_{k_0}, \forall k_0\}$

the use of these L harmonic design coordinates is sufficient under time translates to be a basis for the corresponding
15 subspace of V . This means these waveforms provide a complete set of coordinates to describe this subspace. We will use the theorems of Karhunen-Loeve and Mercer and will limit the demonstration to the dc waveform for simplicity and without loss of generality. We start by considering the expansion of a random
20 complex sequence $\{z(n), \forall n\}$ in a series of waveform coordinates consisting of time translates of the mother waveform ψ . The sequence $\{z(n), \forall n\}$ is a zero-mean stationary random process which is orthonormal over the sample interval "M" and has a frequency spectrum which is flat and extends over the frequency
25 range $1/LT$ which is centered at baseband corresponding to a zero frequency. This means the $\{z(n), \forall n\}$ cover the subspace of V corresponding to the scale of our ~~new~~-dc waveform ψ and its time translates $\{\psi(n-qM) = \psi_q(n), \forall q\}$. In addition, the V is now considered to be extended over a time interval which is
30 relatively large compared to the N-dimensional t-f space in FIG.

1,2 to avoid end-effects on the analysis. We start by approximating the sequence $\{z(n), \forall n\}$ by the $\{\hat{z}(n), \forall n\}$ where:

$$\begin{aligned}\hat{z}(n) &= \sum_q Z_q \psi(n - qM) \\ &= \sum_q Z_q \psi(n_0 + (n_1 - q)M)\end{aligned}$$

where the complex coefficients $\{Z_q\}$ are

$$\begin{aligned}Z_q &= \sum_n z(n) \psi^*(n - qM) \\ &= \sum_n z(n) \psi_q(n)\end{aligned}\tag{12}$$

The following equations prove that the coefficients $\{Z_q, \forall q\}$ are orthonormal:

$$\begin{aligned}Z_q Z_{q'}^* &= \sum_{\Delta n} z(\Delta n - qM) z^*(\Delta n - q'M) \psi_q(\Delta n) \psi_{q'}^*(\Delta n) \\ &= \delta_{qq'} \sum_n |\psi_q(n)|^2 \text{ since the sequence } \{z\} \text{ is orthonormal} \\ &\quad \text{for } qM \text{ time translates} \\ &= \delta_{qq'} \text{ with normalization of the energy of } \psi\end{aligned}\tag{13}$$

Equations (12) and (13) together prove the Karhunen-Loeve's theorem which proves the following equation for the accuracy in approximating the stochastic sequence $\{z(n), \forall n\}$ by $\{\hat{z}(n), \forall n\}$. This accuracy is expressed by the expected "E(o)" squared error "(o)" in this approximation:

$$E\{z(n) - \hat{z}(n)\}^2 = 1 - \sum_{n_1} |\psi(n_0 + n_1 M)|^2 \quad (14)$$

We need to prove that the right hand side of this equation is zero which then proves that the approximating sequence is equal to the original sequence in the mean-square sense. In turn this proves that the new waveform coordinates $\{\psi_q, \forall q\}$ are a basis for the original sequence $\{z(n), \forall n\}$ which is our goal.

The right hand side of equation (14) when set equal to zero expresses Mercer's theorem so our goal is to prove Mercer's theorem. To do this we use the DFT of ψ in equation (11) and the coordinates in (10) to evaluate the right hand side of equation (14). We find

$$1 - \sum_{n_1} |\psi(n + n_1 M)|^2 = 1 - \sum_{k_0} \sum_{k_0'} \Psi_{k_0} \Psi_{k_0'}^* W_N^{\Delta k_0 n_0} \Gamma$$

where $\Gamma = (1/L) \sum_{n_1} W_L^{\Delta k_0 n_1}$

$$= \sin(\pi \Delta k_0) / L \sin(\pi \Delta k_0 / L)$$

$$= 1 \text{ for } \Delta k_0 = 0$$

$$= 0 \text{ otherwise} \quad \text{_____ (15)}$$

This proves that

$$1 - \sum_{n_1} |\psi(n + n_1 M)|^2 = 0 \quad \forall n_0$$

which proves that equation ~~(14)~~ (14) reduces to

20

$$E\{z(n) - \hat{z}(n)\}^2 = 0 \quad \text{_____ (16)}$$

which as per the above proves that the set of multi-resolution waveforms is a basis. This proof easily generalizes to the multi-resolution waveforms at all of the scales $\{p\}$ and time translates $\{q\}$, and to the expansion of the harmonic design coordinates over $2L, 3L, \dots$ as required by the application.

~~New~~ Our new waveforms have multi-scale properties that we will demonstrate. We start with the observation that the Fourier domain design ~~for the new waveforms~~ provides a natural and easy way to derive the complete set of waveforms $\{\psi_{p,q}, \forall p,q\}$ for the space V from the design of the dc waveform ψ by using the same invariant set of Fourier domain harmonic design coordinates $\{\Psi_{k_0}, \forall k_0\}$ derived for the dc multi-resolution waveform. This demonstration requires that we show 1) how the multi-scale transformations are implemented with the design in the Fourier domain, and 2) how the waveform design remains invariant under scale changes.

First consider the multi-scale transformation which derives the waveforms at the scale and shift parameters " p,q " ~~for~~ from the dc waveform at scale " $p=0$ " and centered at the origin " $q=0$ ". We begin by extending the parameters and coordinates in equation (10), to include both scaling and subsampling or decimation in a form that is equivalent to the iterated filter bank construction which is used to derive ~~the~~ current Wavelet waveforms using the filter scaling functions. Starting with the coordinates at scale " $p=0$ " the parameters and coordinates at scale " $p=p$ " are given by the equations:

$$\begin{aligned}
 & \underline{p=0} \quad \text{parameters and coordinates} \\
 & n = n_0 + n_1 M \\
 & n_0 = a_0 + a_1 2 + \dots + a_{m-1} 2^{m-1}
 \end{aligned}
 \tag{17}$$

$$\begin{aligned}
&= M \text{ points} \\
M &= 2^m \\
n_1 &= b_0 + b_1 2 + \dots + b_{l-1} 2^{l-1} \\
&= L \text{ points spaced at } M \text{ sample intervals} \\
5 \quad \underline{L} &= 2
\end{aligned}$$

$p=p$ parameters and coordinates

$$\begin{aligned}
10 \quad &\text{---} 2^{-p} n(\downarrow 2^p) = \text{scaled by "2}^{-p}\text{"} \\
&\text{and subsampled or decimated by } 2^p:1 \\
&= n_0(p) + n_1(p)M \\
&2^{-p} n_0(\downarrow 2^p) = \text{scaled by "2}^{-p}\text{"} \\
&\text{and subsampled or decimated by } 2^p:1 \\
&= n_0(p) \\
&= a_p + a_{p+1}2 + \dots + a_{p+m-1} 2^{p+m-1} \\
15 \quad &= M \text{ points spaced at } 2^p \text{ sample intervals} \\
&2^{-p} n_1(\downarrow 2^p) = \text{scaled by "2}^{-p}\text{"} \\
&\text{and subsampled or decimated by } 2^p:1 \\
&= n_1(p) \\
&= b_p + b_{p+1} 2 + \dots + b_{p+l-1} 2^{p+l-1} \\
20 \quad &= L \text{ points spaced at } M2^p \text{ sample intervals}
\end{aligned}$$

25 together with the observation that the sampling interval "T" is
 increased to " $2^p T$ " under the scale change from " $p=0$ " to " $p=p$ " and
 subsampling or decimation from " $1:1$ " to " $2^p:1$ ". Combining these
 equations with the analytical formulation in (7) and the Fourier
 domain representation in (11) enables the waveforms at the
 parameters " p, q " to be written as a function of the Fourier
 domain harmonic design coordinates:

30

$$\begin{aligned}\psi_{p,q,r}(n) &= 2^{-p/2} \psi(2^{-p}n - qM) e^{i2\pi f_c(p,r)nT} \\ &= (2^{-p/2} / N') \sum_{k_0} \Psi_{k_0} W_{N'}^{k_0(n(p)-qM)} e^{i2\pi f_c(p,r)n(p)2^p T}\end{aligned}\quad (18)$$

for all admissible scale, translation, and frequency index
5 parameters "p,q,r".

Next we need to demonstrate that the frequency domain
design in (11) remains invariant for all parameter changes and in
particular for all scale changes. This multi-scale property
10 expresses the accordion behavior of the design in that the
Wavelets at different scales are simply the stretched and
compressed versions of the mother waveform with the appropriate
frequency translation indices. This multi-scale invariancy means
that the design for a M=16 channel filter bank remains the same
15 for M=100 or M=10,000 channel filter banks, when the overlap L
and the performance goals remain constant. To demonstrate this
invariant property across scales, we consider the ~~mr~~-multi-
resolution waveform at scale "p" with the other parameters set
equal to zero for convenience "q=0, r=0" and without loss of
20 generality. The Fourier domain frequency response $\Psi(f)$ can be
evaluated starting with the original formulation in equation (7):

25

$$\text{DFT at "p, q=0, r=0"} \quad (19)$$

$$\begin{aligned}
\Psi_p(f) &= (1/N') \sum_{k_0} \Psi_{k_0} \sum_{n(p)} W_{N'}^{-(fN'2^p T - k_0)n(p)} \\
&= \sum_{k_0} \Psi_{k_0} \left[\frac{\sin(\pi (fN'2^p T - k_0))}{N' \sin(\pi (fN'2^p T - k_0)/N')} \right] \\
&= \sum_{k_0} \Psi_{k_0} [\text{Harmonic interpolation for "k}_0\text{"}]
\end{aligned}$$

This only differs from the harmonic representation in equation
 5 **(9)** in the restriction of the design coordinates to the subset of
 harmonic coefficients $\{\psi_{k_0}, \forall k_0\}$ and the stretching of the time
 interval to " $2^p T$ " corresponding to the scale " $p=p$ ". The harmonic
 interpolation functions are observed to remain invariant over
 scale changes upon observing that the frequency scales as
 10 " $f \sim 1/2^p T$ " which means the "frequency*time" product remains
 invariant with scale changes as per the fundamental property of
 the waveforms. This means the harmonic interpolation functions
 remain invariant with scale change and therefore the frequency
 response remains an invariant. This demonstrates the waveform
 15 design is an invariant across the waveform scales which means we
 only need a single design for all scales or resolutions of
 interest.

LS design algorithms for new waveform will be described to
 20 illustrate the advantages our ~~new~~ waveform has over current
 designs. The two LS algorithms described are the eigenvalue and
 the gradient search which respectively can be reduced to
 algorithms which are equivalent to ~~the original current~~
 eigenvalue [7] and Remez-exchange [8] waveform design algorithms
 25 for application to a uniform filter bank. We consider the t-f
 space which is spanned by a uniform polyphase filter bank
 consisting of M channels at the frequency spacing $f_w = 1/MT$ where T
 is the digital sampling interval, and the filter waveform FIR

time response is stretched over L sampling time intervals T_s . This polyphase filter bank is ideally decimated which means the filter output sample rate $1/T_s$ is equal to the channel-to-channel spacing $1/T_s = 1/MT$, equivalent to stating that there is no excess bandwidth $\alpha=0$. Our design for this topology is immediately applicable to an arbitrary set of multi-resolution filters through the scaling equation (18) which gives the design of our waveform at arbitrary scales in terms of our design of the dc waveform.

For this polyphase filter bank used to construct the dc waveform or filter impulse response, our LS example design algorithms will use 5 metrics consisting of the 2 prior art passband and stopband metrics, and the 3 new metrics consisting of the ISI, ACI, and QMF, and solve the LS minimization problem using as design coordinates the subset of harmonic coordinates which are a basis. Since our ~~2~~-two example LS design algorithms only differ in the use of an eigenvalue LS optimization and the use of a gradient search LS optimization, the flow diagrams for the construction of the cost functions and the solution for the optimal waveform will be identical. However, there are differences in the construction of the cost functions from the respective metrics and in the iterative solution mathematics. Both LS solutions for the harmonic design coordinates minimize the weighted sum of the error residuals or cost functions from the 5 metrics. These design coordinates ~~for~~ are the Fourier harmonics $\{\psi_{k_0}, \forall k_0\}$ for $\{k_0 = 0, 1, \dots, L-1\}$. Resulting algorithms are easily extended to the applications requiring the design coordinates to cover $2L, 3L, \dots$ harmonics.

Frequency domain design coordinates are related to the waveform time domain digital samples or coordinates as follows.

Mappings of ~~time~~ \leftrightarrow frequency to time _____ (20)

Time domain design coordinates $\{\psi(n), \forall n\}$ are real and symmetric and can be represented by the reduced set $\{h_t(n), n=0, 1, \dots, ML/2\}$

$$\begin{aligned} h_t(n) &= \psi(0) \quad \text{for } n=0 \\ &= 2\psi(n) \quad \text{for } n=1, 2, \dots, ML/2 \\ &= \text{time domain design coordinates} \end{aligned}$$

Frequency domain harmonic design coordinates $\{\psi_{k_0}, \forall k_0\}$ are real and symmetric and can be represented by the reduced set $\{h_f(k), k=0, 1, \dots, L-1\}$

$$\begin{aligned} h_f(k) &= \psi_{k_0} \quad \text{for } k=k_0=0 \\ &= 2\psi_{k_0} \quad \text{for } k=k_0=1, 2, \dots, L-1 \\ &= \text{frequency domain design coordinates} \end{aligned}$$

Mapping of the frequency coordinates $\{h_f(k), k=0, 1, \dots, L-1\}$ into the time coordinates $\{h_t(n), n=0, 1, \dots, ML/2\}$ is defined by the matrix transformation to within a scale factor

$$h_t = B h_f$$

where

$$\begin{aligned} h_f &= (h_f(0), \dots, h_f(ML/2))^t \quad \text{transpose of column vector} \\ h_t &= (h_t(0), \dots, h_t(ML/2))^t \quad \text{transpose of column vector} \\ B &= (ML/2 + 1) \times L \quad \text{matrix} \\ &= [B_{kn+1, k+1}] \quad \text{matrix of row } k \text{ and column } n \end{aligned}$$

$$\begin{aligned} &\text{elements } B_{kn} \\ B_{kn+1, k+1} &= 1/ML \quad \text{for } n=1 \\ &= 2 \cos(2\pi kn/ML) \quad \text{otherwise} \end{aligned}$$

~~Mappings of the frequency coordinates $\{h_f(k), k=0, 1, \dots, L-1\}$ into the time coordinates $\{h_t(n), n=0, 1, \dots, ML/2\}$ and vice versa are defined by the matrix transformations~~

~~$$h_t = B h_f$$~~

$$\underline{h_f} = B^{-1} \underline{h_t}$$

where

$$\underline{h_f} = (h_f(0), \dots, h_f(ML/2))^t \text{ --- transpose of column vector}$$

$$\underline{h_t} = (h_t(0), \dots, h_t(ML/2))^t \text{ --- transpose of column vector}$$

$$B = (ML/2 + 1) \times L \text{ --- matrix}$$

$$= [B_{kn}] \text{ --- matrix of row } k \text{ and column } n \text{ elements } B_{kn}$$

$$B_{kn} = 1 / (ML + 1) \text{ --- for } n=1$$

$$= 2 \cos(2\pi kn / (ML + 1)) \text{ --- otherwise}$$

$$B^{-1} = L \times (ML/2 + 1) \text{ --- matrix}$$

$$= [B_{kn}^{-1}] \text{ --- matrix of row } k \text{ and column } n \text{ elements } B_{kn}^{-1}$$

$$B_{kn}^{-1} = 1 \text{ --- for } n=1$$

$$= 2 \cos(2\pi kn / (ML + 1)) \text{ --- otherwise}$$

and

$$B^{-1} B = I \text{ --- } L \times L \text{ identity matrix}$$

$$B B^{-1} = I \text{ --- } (ML/2 + 1) \times (ML/2 + 1) \text{ identity matrix}$$

wherein $N' = ML + 1$ has been replaced by ML since a single end point has been added to the FIR to make it symmetrical for ease of implementation.

20

Passband and stopband metrics and cost functions are derived with the aid of FIG. 3 which defines the power spectral density (PSD) parameters of interest for the passband and stopband of the PSD $\Psi(\omega)$ for communications applications. Requirements for radar applications include these listed for communications. Referring to FIG. 3 the passband 11 of the waveform PSD is centered at dc ($f=0$) since we are designing the dc or baseband waveform, and extends over the frequency range ω_p extending from $-\omega_p/2$ to $+\omega_p/2$ 12 in units of the radian frequency variable $\omega = 2\pi fT$ 13 where T is the digital sampling interval defined in FIG. 1. The frequency space extends over the range of $f = -1/2T$ to $f = +1/2T$ which is the frequency range in

FIG 1 translated by $-1/2T$ so that the dc waveform is at the center of the frequency band. Quality of the PSD over the passband is expressed by the passband ripple 14. Stopband 15 starts at the edge 16 of the passbands of the adjacent channels $\pm\omega_a/2$ 16 and extends to the edge of the frequency band $\omega=\pm\pi$ 17 respectively. Stopband attenuation 18 at $\pm\omega_a/2$ measures the PSD isolation between the edge of the passband for the dc waveform and the start of the passband for the adjacent channels centered at $\pm\omega_s$ 19. Rolloff 20 of the stopband is required to mitigate the spillover of the channels other than the adjacent channels, onto the dc channel. Deadband or transition band 21 is the interval between the passbands of contiguous channels, and is illustrated in FIG. 3 by the interval from $\omega_p/2$ to $\omega_a/2$ between the dc channel and adjacent channel at ω_a . Waveform sample rate ω_s 22 is the waveform repetition rate. For the LS example algorithms, the waveform sample rate is equal to the channel-to-channel spacing for zero excess bandwidth. Therefore, $1/T_s = \omega_s/2\pi T = 1/MT$ which can be solved to give $\omega_s = 2\pi/M$ for the radian frequency sampling rate of the filter bank which is identical to the waveform repetition rate.

We start by rewriting the DFT equations for the dc waveform in (11) as a function of the $\{h_f(k), k=0,1,\dots,L-1\}$

$$\begin{aligned} \psi(\omega) &= \sum_n \psi(n) \cos(n\omega) \\ &= \mathbf{c}^T \mathbf{B} \mathbf{h}_f \quad \text{using (20) and the definition of the vector "c"} \\ \mathbf{c} &= (1, \cos(\omega), \dots, \cos((ML/2)\omega))^T \text{ transpose of column vector} \end{aligned} \tag{21}$$

which is equivalent to the equation for $\psi(\omega)$ in (9) expressed as a linear function of the $\{h_f(k), k=0,1,\dots,L-1\}$. However, this functional form suggested by the eigenvalue formulation [7]—is more convenient to analyze. An ideal "c" vector " \mathbf{c}_r " will be

introduced for the passband and the stopband in FIG. 3, in order to identify the error residual $\delta\psi(\omega)$ at the frequency " ω " in meeting the ideal passband and stopband requirements. The ideal PSD is flat and equal to "1" for the passband, and equal to "0" for the stopband. We find

Error residuals for passband and stopband (22)

$$\begin{aligned} c_r &= (1, 1, \dots, 1)^t \quad \text{passband ideal "c"} \\ &= (0, 0, \dots, 0)^t \quad \text{stopband ideal "c"} \\ \delta c &= c_r - c \quad \text{error vector} \\ \delta\psi(\omega) &= \delta c^t B h_f \\ &= \text{Residual error in meeting the ideal spectrum at "}\omega\text{"} \end{aligned}$$

The LS metric for the passband and stopband can now be constructed as follows for the eigenvalue and the LS optimization ~~(or equivalently, the LS algorithm) design algorithms.~~

Passband and stopband metrics (23)

$$\begin{aligned} J(\text{band}) &= \frac{1}{\text{band}} \int_{\text{band}} |\delta\psi(\omega)|^2 d\omega \quad \text{Eigenvalue} \\ &= h_f' R h_f \quad \text{Eigenvalue} \\ &= \|\delta\psi\|^2 \quad \text{LS} \end{aligned}$$

~~(23) continued~~

—where

$$\begin{aligned} \text{band} &= [0, \omega_p) \quad \text{passband} \\ &= (\omega_s, \pi] \quad \text{stopband} \end{aligned}$$

$$\begin{aligned}
\mathbf{R} &= \frac{1}{\text{band}} \int_{\text{band}} (\mathbf{B}' \delta \mathbf{c} \delta \mathbf{c}' \mathbf{B}) d\omega \\
&= L \times L \text{ matrix} \\
\delta \psi &= (\delta \psi(\omega_1) , \dots , \delta \psi(\omega_u))^t \\
&= \text{vector of error residuals at the} \\
&\quad \text{frequencies } \omega_1 , \dots , \omega_u \text{ across the band} \\
\|(\mathbf{o})\| &= \text{norm or length of the vector } (\mathbf{o}) \text{ and which} \\
&\quad \text{includes a cost function for the errors of} \\
&\quad \text{the individual components}
\end{aligned}$$

where it is observed that the eigenvalue approach requires that the LS metrics be given as quadratic forms in the design coordinates $\{h_f(k), k=0,1,\dots,L-1\}$ whereas with the LS approach it is sufficient to give the LS metrics as squared vector norms with imbedded cost functions or an equivalent formulation.

QMF metrics express the requirements on the deadband that the PSD's from the contiguous channels in FIG. 3 add to unity across the deadband $[\omega_p, \omega_s]$ in order that the filters be QMF filters. By suitable modification of the error vector $\delta \mathbf{c}$, the previous construction of the passband and stopband metrics can be modified to apply to the deadband. This is a Wavelet requirement on the frequency coverage of the Wavelet basis ~~as observed in Table 1.~~ We find

Deadband metrics (24)

$$J(\text{deadband}) = \frac{1}{\text{deadband}} \int_{\text{deadband}} \|\delta \psi(\omega)\|^2 d\omega \quad \text{Eigenvalue}$$

(24) continued

$$\begin{aligned} &= h_f' \mathbf{R} h_f && \text{Eigenvalue} \\ &= \|\delta\psi\|^2 && \text{--LS} \end{aligned}$$

where

5 $\delta c = c_r - c(\omega) - c(\pi/M - \omega)$

where $c(\omega)=c$ as defined in (22) and (23), and $c(\pi/M - \omega) = c$ at the offset frequency " $\pi/M - \omega$ " corresponding to the overlap of the contiguous filters over the deadband.

10

Orthonormality metrics measure how close we are able to designing the set of waveforms to be orthonormal over the t-f space, with the closeness given by the ISI and the ACI. ~~ISI is the non-orthogonality error between channel output samples separated by multiples of the sampling interval $1/MT$ seconds where T is the sample time and M is the interval of contiguous samples. ACI is the non-orthogonality error between channel output samples within a channel and the samples in adjacent channels at the same sample time and at sample times separated by multiples of the sample interval. As observed as noise contributions within each sample in a given channel, the ISI is the noise contribution due to the other received waveforms at the different timing offsets corresponding to multiples of the sampling interval. Likewise, the ACI is the noise contribution due to the other waveforms in adjacent channels at the same sampling time and at multiples of the sampling interval.~~

15

20

25

ISI and ACI errors are fundamentally caused by different mechanisms and therefore have separate metrics and weights to specify their relative importance to the overall sum of the LS metrics. ISI is a measure of the non-orthogonality between the stream of waveforms within a channel as per the construction in FIG. 3. On the other hand, ACI is a measure of the non-

30

orthogonality between the waveform within a channel and the other waveforms in adjacent channels. This means the stopband performance metric has a significant impact on the ACI due to the sharp rolloff in frequency of the adjacent channel, ~~and the~~
 5 ~~ACI metric is then a measure of the residual non-orthogonality due to the inability of the stopband rolloff in frequency from completely eliminating the ACI errors.~~

We assume that the received waveform is identical to the
 10 filter waveforms and is transmitted at the filter output sample intervals equal to $1/MT$ seconds. The second assumption means we are assuming the receiver is synchronized with the received signal. ~~Since there is no information lost by sampling asynchronously with the received waveform, we are free to make~~
 15 ~~this synchronization assumption without loss of generality.~~ ISI metrics are derived in the following set of equations.

ISI metrics (25)

20 Mapping of h_f into ψ

$$\Psi' = (\psi(-ML/2), \dots, \psi(ML/2))^t \text{ transpose of}$$

column vector Ψ

$$= H h_f$$

$$H = (ML+1) \times L \quad \text{matrix of elements } H_{kn} = H_{m, k+1}$$

25 $H_{kn} = H_{m, k+1} = 1 \quad \text{for } nk = \pm 0$

$$= 0.5 \cos(2\pi kn/ML+1) \quad \text{otherwise}$$

$$\text{where } m = n + ML/2 + 1$$

Offset matrix A

30 $A = L \times (ML+1) \quad \text{matrix of elements } A_{k+1, n-m}$

$$A_{k+1, nm} = [0 \ 0 \ \dots \ 0 \quad 0] \text{ row vector } k=00$$

~~for $k=1$~~

$$= [0 \quad -0 \quad \dots \quad -\psi(-ML/2) \quad \dots \quad -\psi((L-k)M+1)] \quad \text{row vector } k+1$$

(25) continued

$$\begin{array}{ccccccc} 1 & 2 & & kM & & LM+1 & \text{column } m \text{ element} \\ & & & & & & \text{of row vector} \end{array}$$

5

ISI error vector δE

$$\begin{aligned} \delta E &= L \times 1 \quad \text{column vector} \\ &= A H h_f \end{aligned}$$

10

ISI metric

$$\begin{aligned} J(\text{ISI}) &= \delta E^t \delta E && \text{Eigenvalue} \\ &= \text{Non-linear quadratic function of } h_f \\ &= \|\delta E\|^2 && \text{LS} \end{aligned}$$

15

ACI metrics are derived using the ISI metric equations with the following modifications.

ACI metrics (26)

20

Mapping of h_f into ψ is the same as developed for ISI
Offset matrix A elements are changed as follows to apply to
Channel 1:

$$\begin{aligned} A_{kn} &= [0 \quad 0 \quad \dots \quad 0 \quad \dots \quad 0] \quad \text{for row vector } k=10 \\ &= [0 \quad 0 \quad \dots \quad \psi(-ML/2) W_M^0 \quad \dots \quad \psi((L-k)M+1) W_M^{(L-k)}] \quad \text{row} \\ &\quad \text{vector } k+1 \end{aligned}$$

$$\begin{array}{ccccccc} 1 & 2 & & kM+1 & & LM+1 & \text{column } m \text{ element} \\ & & & & & & \text{of row vector} \end{array}$$

which means the ACI error vector δE is

30

$$\begin{aligned} \delta E &= L \times 1 \quad \text{column vector} \\ &= A H h_f \end{aligned}$$

ACI metric for the two contiguous channels

$$\begin{aligned}
J(\text{ISI}) &= 2 \delta E^t \delta E && \text{Eigenvalue} \\
&= \text{Non-linear quadratic function of } h_f \\
&= 2 \|\delta E\|^2 && \text{LS}
\end{aligned}$$

5 where the factor "2" takes into account there are two contiguous
channels or one on either side of the reference channel 0 in FIG.
3. Because of the fast rolloff of the frequency spectrum the
addition of more channels into the ACI metric is not considered
necessary, although the functional form of the ACI metric in (26)
10 allows an obvious extension to any number of adjacent channels
which could contribute to the ACI.

Cost function J for the LS algorithms is the weighted sum
of the LS metrics derived in (23), (24), (25), (26). The LS
15 algorithms minimize J by selecting the optimal set of frequency
coordinates $\{h_f(k), \forall k\}$ for the selected set of parameters used
to specify the characteristics of the dc waveform, frequency
design coordinates, LS metrics, and weights. Cost function and
optimization techniques are given by the equations

20

Cost function J (27)

$$\begin{aligned}
J &= \sum_x w(\text{metrics}) J(\text{metrics}) \\
&= \text{weighted sum of the LS metrics } J(\text{metrics})
\end{aligned}$$

25

where

metrics = passband, stopband, deadband, ISI, ACI
 $\{w(\text{metrics}), \forall \text{metrics}\}$ = set of weights

$$\sum_x w(\text{metrics}) = 1 \quad \text{normalization}$$

30

Optimization goal

Goal: minimize J with respect to the selection of
the $\{h_f(k), \forall k\}$

Optimization algorithms

Two algorithms are the Eigenvalue and the LS optimization
5 where the eigenvalue optimization algorithm uses the non-
linear quadratic formulations of the LS metrics and the LS
optimization algorithm uses the squared norm formulations
for the LS metrics.

10

FIG. 4 is a summary of the LS metrics and the construction
of the cost function J . Design parameters **23** ~~are the input and~~
~~output design parameters. Input parameters are L , the number of~~
~~polyphase channels M , or equivalently the number of digital~~
15 ~~samples at spacing T over the symbol interval $T_s = MT$, the length~~
~~of the FIR time response for the waveform in units of L which are~~
~~the number of digital samples per waveform repetition interval T_s~~
~~so that the total number of digital samples for the symmetric FIR~~
~~time response is equal to $N' = ML + 1$, number of DFT samples per FIR~~
20 ~~length n_{fft} for implementation of the LS algorithms, passband~~
~~radian frequency ω_p , stopband radian frequency ω_a , waveform~~
~~repetition rate in radian frequency ω_s , selection of the set of~~
~~design coordinates $\{h_f\}$ to be used in the optimization, and the~~
~~metric weights $\{w(\text{metrics})\}$. Output parameters are the set of~~
25 ~~harmonic design coordinates $\{h_f\}$ that minimize J . Band metrics~~
~~**24** are the passband, stopband, and deadband metrics defined in~~
~~equations **(23)**, **(23)**, **(24)** respectively. Interference metrics~~
~~**25** are the ISI and ACI metrics defined in equations **(25)** and~~
~~**(26)** respectively. LS cost function J **26** is the weighted~~
30 ~~linear sum of the metrics defined for the band **24** and the~~
~~interference **25** as defined in equation **(27)**.~~

FIG. 5 is a flow diagram of the LS recursive solution
algorithm. There are two loops with the topology constructed so

that the outer loop **27** is an iteration over the set of metric weights $\{w(\text{metrics})\}$, and the inner nested loop **28** is the recursive or iterated LS solution to find the optimal $\{h_f\}$ for the given design parameters and weights where each step refers to an iteration step in the solution. A recursive LS solution is required to be able to solve the highly non-linear interference metrics as well as the band metrics when one chooses to use non-linear techniques to construct these metrics.

10

15

Consider the inner nested loop **28**. The recursive LS solution starts with the initial step $i=0$ **29** which begins with the selection of the input design parameters and weights and the selection of an initial set of values for the $\{h_f\}$ **30**. Next the band metrics are calculated **31**. Since this is the initial step $i=0$ **32** the cost function J is restricted to the linear band metrics in order to find the linear approximation to $\{h_f\}$ **33** to initialize the non-linear solution starting with step $i=1$ **34** wherein the highly non-linear interference metrics are included in J . Following the signal flow, for step $i=1$ the band metrics **31** and interference metrics **35** are calculated, weighted, and summed to form the cost function J **36**. An iterative solution algorithm **37** finds the best approximation in step $i=1$ to the $\{h_f\}$ which minimizes J using the approximation to $\{h_f\}$ from the previous step $i=0$ to linearize the search algorithm coefficients for the eigenvalue and LS step $i=1$ iteration. If there is no convergence to the correct solution for $\{h_f\}$ this recursive sequence of calculations is repeated for step $i=2$ **34**. This recursive solution technique is repeated for subsequent steps

until there is convergence 38 whereupon one exits this inner loop.

Consider the outer loop. After exiting the inner loop 38
5 the solution for $\{h_f\}$ is tested to see if it meets the performance goals 39. If not, a new set of metric weights is selected and the inner loop is initialized $i=0$ 40 and the inner loop is used to find the next solution for $\{h_f\}$. This process continues until the performance goals are met or
10 adequated approximated 39 whereupon the algorithm is exited with the final solution set $\{h_f\}$ 41.

Applications of this new invention to both communications and radar will be given using these example algorithms and other
15 algorithms supported by this invention. These new waveforms are considered for the applications: 1) to replace the square-root raised cosine waveform (sq-root rc) which is extensively used for the third generation (3G) CDMA communications, 2) to replace the Gaussian minimum shift keying (GMSK) waveform for constant
20 amplitude bandwidth efficient (BEM) applications, and 3) as a candidate waveform for synthetic aperture radar (SAR) and real aperture radar (RAR) applications.

CDMA communications applications for the current and the
25 new 3G CDMA considers the use of a waveform designed with this new invention as a possible replacement for the sq-rt rc waveforms with bandwidth expansion parameter $\alpha=0.22$ to $\alpha=0.40$. This notation means that for $\alpha=0.22$ the spectral efficiency is (symbol rate/bandwidth) = $1/1+\alpha = 1/1.22 = 0.82 = 82\%$. A basic
30 advantage of the our waveform for 3G CDMA is the potential for a symbol rate increase within the same bandwidth with an increase in the spectral efficiency to $\approx 100\%$ depending on the application and operational constraints. The dc power spectral density or power spectrum (PSD) of the waveform is compared to the PSD for

the sq-rt r-c in FIG. 6. Plotted are the measured PSD in dB 42
versus the frequency offset from dc expressed in units of the
symbol rate 43 Plotted against the normalized frequency offset
are the dc PSD for the new waveform 44, the sq-rt r-c with
5 $\alpha=0.22$ 45, and the sq-rt r-c with $\alpha=0.40$ 46. It is observed
that the PSD for the new waveform rolls off faster than that for
the sq-rt r-c which means that the new ~~mr~~-waveform ~~will~~
~~support~~offers the potential for an increased symbol rate for a
given available frequency band. ~~while satisfying the inherent~~
10 ~~requirements for low ISI and MAI (multiple access interference).~~

Constant amplitude BEM application of the new waveform
indicates that it is a viable candidate for replacing the current
preferred modulation waveform which is the GMSK. The GMSK finds
15 applications for transmitters which operate their HPA(s)
amplifiers in a saturation mode in order to maximize their
radiated power from the HPA(s), and which require a BEM PSD to
avoid excessive spreading of the transmitted power. Simulation
data for the dc PSD is plotted in FIG. 7 for the new waveform BEM
20 and the GMSK. Plotted are the measured dc PSD in dB 47 versus
the frequency offset from dc expressed in units of the bit rate
48. ~~Plotted against the normalized frequency offset are the dc~~
~~PSD for the new waveform BEM 49 and the GMSK 50, for a length~~
parameter $L=10$ where L is the length of the phase pulse in terms
25 of the phase pulse repetition rate. ~~The significance of this~~
~~This example data is that the new waveform has~~ indicates the
potential to be designed to ~~of our waveform to~~ offer a PSD which
is less spread out than the current GMSK, and therefore an
improved BEM waveform.

30 Radar RAR and SAR application of the waveform indicates
that it is a viable candidate to replace the current chirp
waveforms for wideband signal transmission, when combined with
pseudo-random phase codes. Results of the simulation for the new

waveform and an unweighted frequency chirp waveform are given in FIG. 8. Plotted are the ambiguity function for the new waveform 51 and the unweighted frequency chirp waveform 52. The dc 2-dimensional radar ambiguity function 53 is plotted as a function of the frequency offset in units of fT_p and the time offset in units of t/T_c where T_p is the phase-coded radar pulse length or length of the phase code and T_c is the phase code chip length. The chip length is identical to the waveform repetition interval T_s so that $T_c = T_s$. ~~It is observed that the~~ This example indicates our new waveform has the potential for ~~significant~~ improvements in the ambiguity function and by implication in the performance.

Preferred embodiments in the previous description ~~is~~ are provided to enable any person skilled in the art to make or use the present invention. The various modifications to these embodiments will be readily apparent to those skilled in the art, and the generic principles defined herein may be applied to other embodiments without the use of the inventive faculty. Thus, the present invention is not intended to be limited to the embodiments shown herein ~~but~~ and ~~is not~~ to be accorded the wider scope consistent with the principles and novel features disclosed herein.

REFERENCES:

- [1] I. Daubechies, "Ten Lectures on Wavelets", Philadelphia:SIAM, 1992
- [2] Ronald R. Coifman, Yves Meyer, Victor Wickerhauser, "Wavelet analysis and signal processing", in "Wavelets and Their Applications", Jones & Bartlett Publishers, 1992

~~[3] T. Blu, "A new design algorithm for two-band orthonormal rational filter banks and orthonormal rational Wavelets", IEEE Signal Processing, June 1998, pp. 1494-1504~~

~~[4] M. Unser, P. Thevenaz, and A. Aldroubi, "Shift-orthogonal Wavelet bases", IEEE Signal Processing, July 1998, pp. 1827-1836~~

~~[5] K.C. Ho and Y. T. Chan, "Optimum discrete Wavelet scaling and its application to delay and Doppler estimation", IEEE Signal Processing, Sept. 1998, pp. 2285-2290~~

~~[6] Q. Pan, L. Zhang, G. Dai, and H. Zhang, "Two denoising methods by Wavelet transforms", IEEE Signal Processing, Dec. 1999, pp. 3401-3406~~

~~[7] P.P. Vaidyanathan and T.Q. Nguyen, "Eigenvalues: A New Approach to Least Squares FIR Filter Design and Applications Including Nyquist Filters", IEEE Trans. on Circuits and Systems, Vo. CAS-34, No. 1, Jan. 1987, pp 11-23~~

~~[8] J.H. McClellan, T.W. Parks and L.R. Rabiner, "A Computer Program for Designing Optimum FIR Linear Phase Filters", IEEE Trans Audio Electroacoust. Vol. AU-21, Dec. 1973, pp. 506-526~~



DRAWINGS AND PERFORMANCE DATA

5

FIG. 1 Wavelet Tiling of an N-Point Digital t-f Space

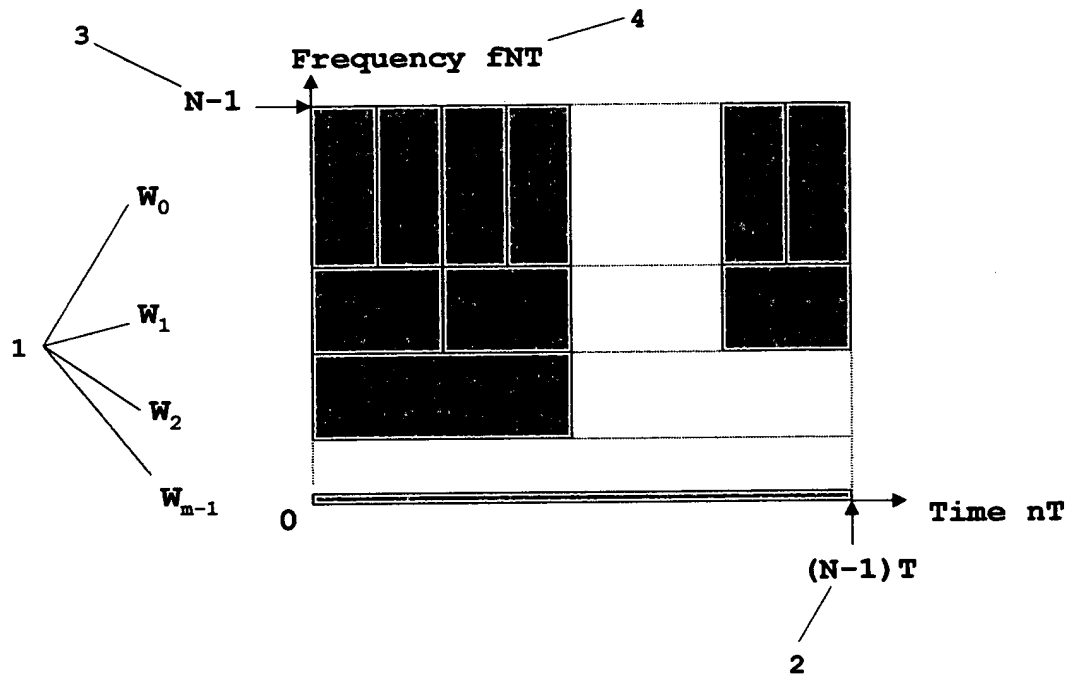
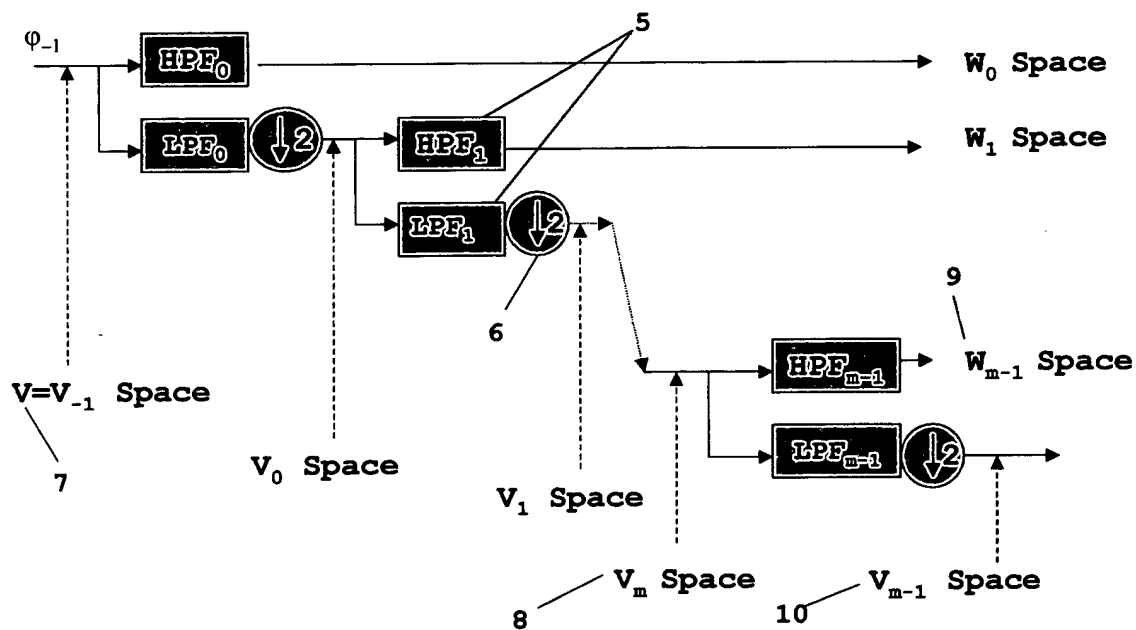


FIG. 2 Wavelet Iterated Filter Bank for Tiling t-f Space in FIG. 1

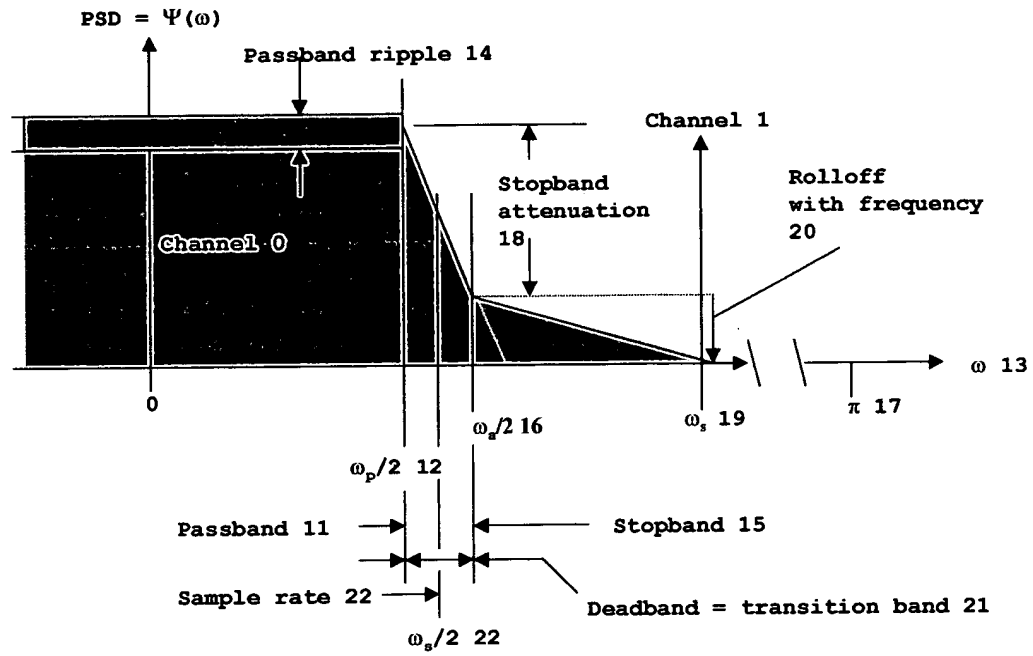


5

10

15

FIG. 3 PSD Requirements for Communications

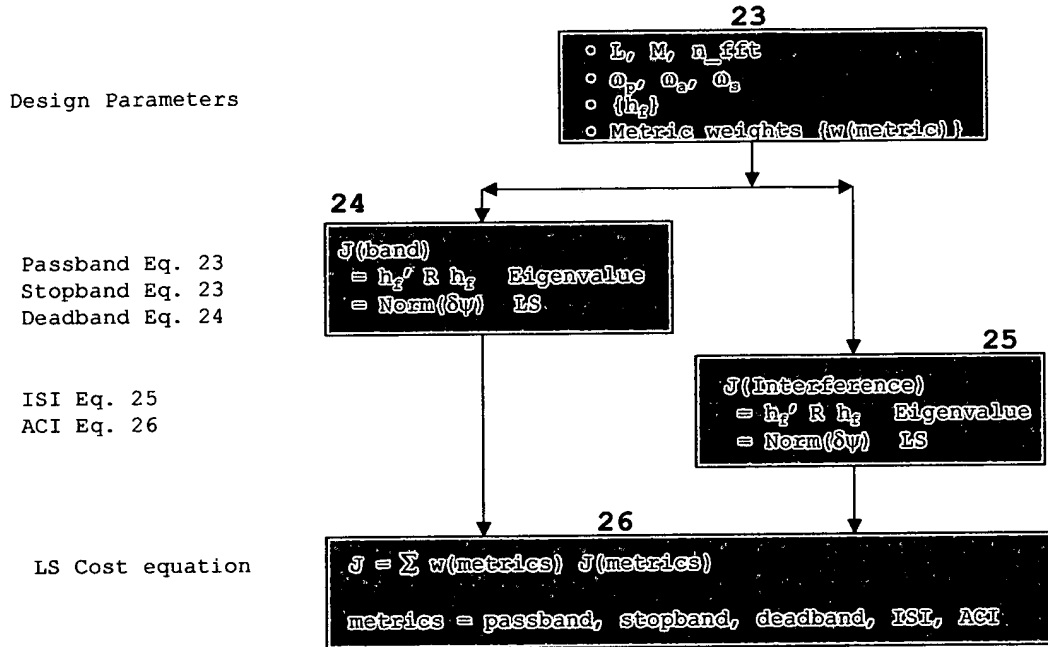


5

10

15

FIG. 4 LS Metrics and Cost Function



5

10

15

FIG. 5 LS Recursive Solution Algorithm

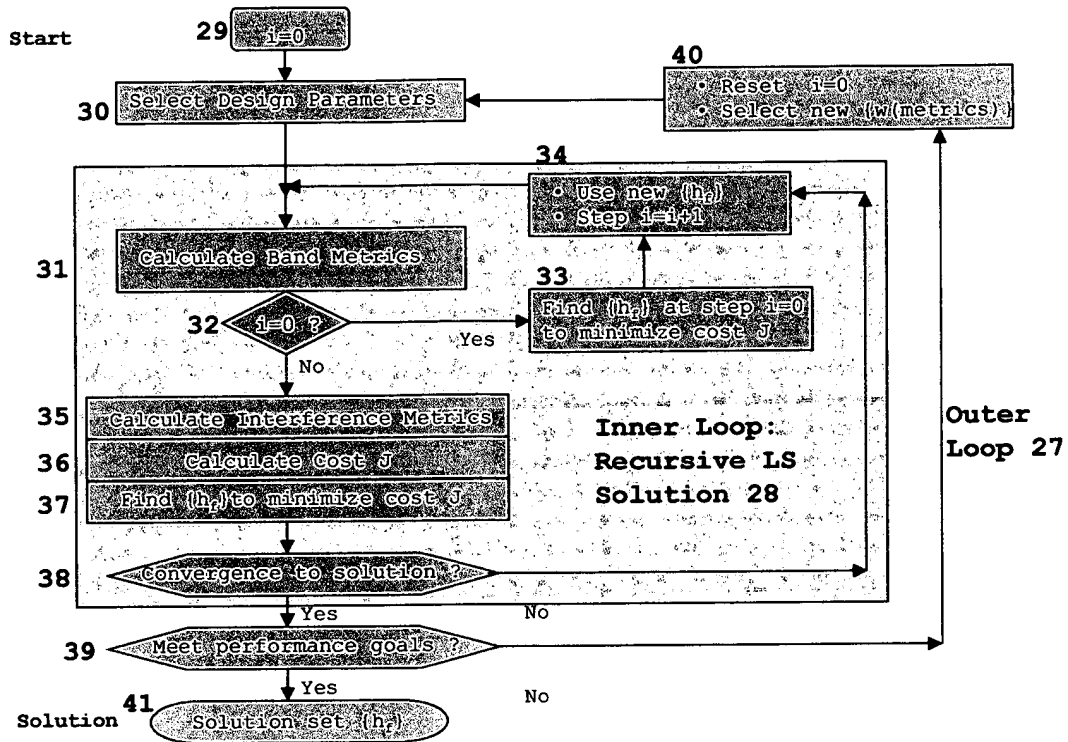
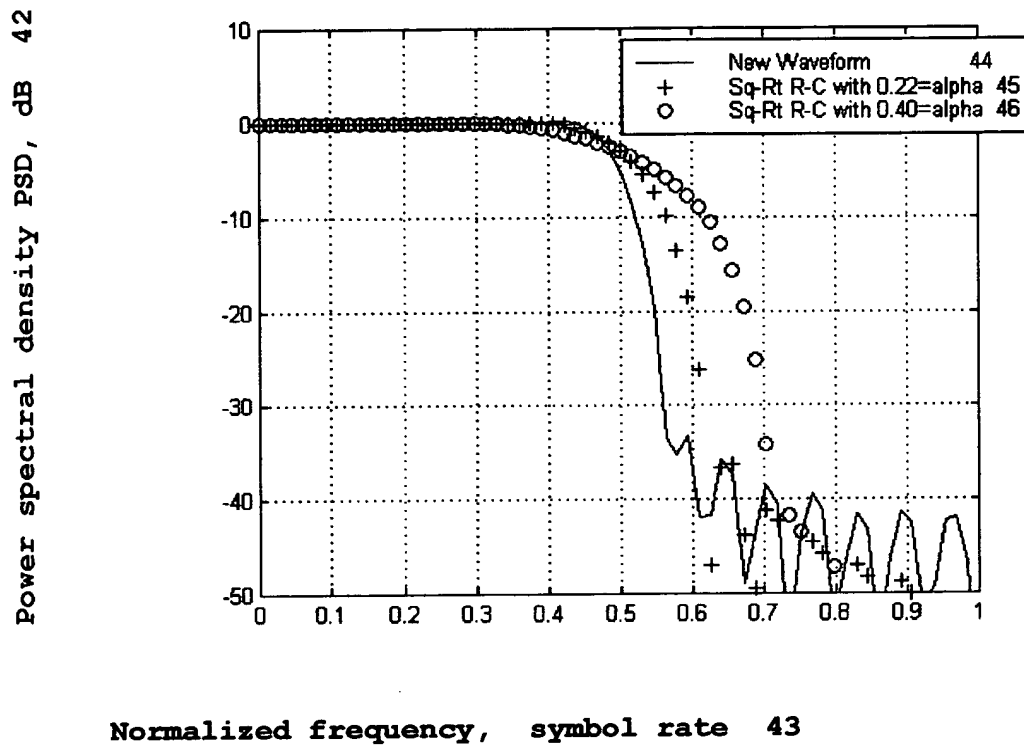


FIG. 6 PSD for New Waveform and Square-Root Raised-Cosine



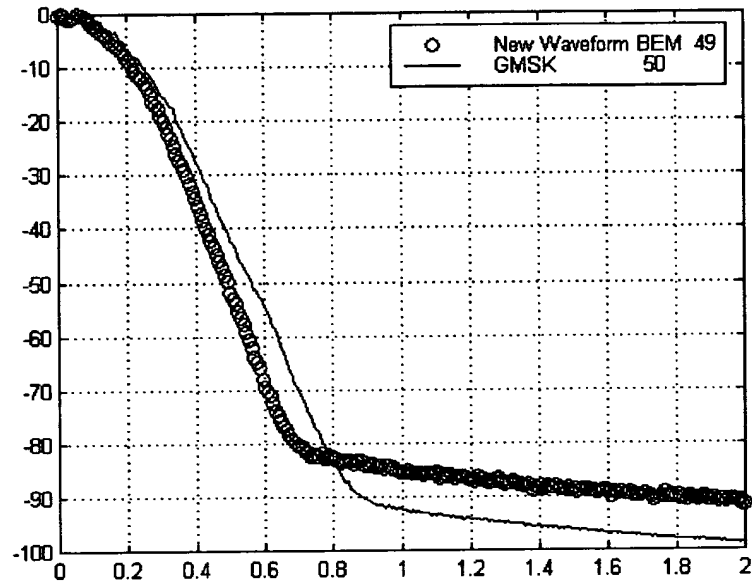
5

10

15

FIG. 7 PSD for New Waveform BEM and GMSK

Power spectral density PSD, dB 47



Normalized frequency, bit rate 48

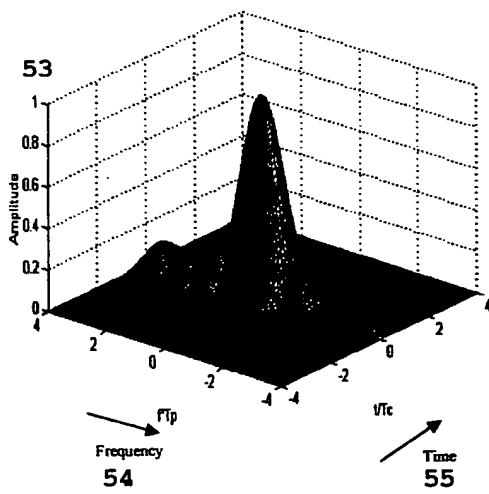
5

10

15

FIG. 8 Radar Ambiguity Functions of New Waveform and Unweighted Chirp Waveform

New Wavelet Ambiguity Function 51



Unweighted Chirp Ambiguity Function 52

